Research Square

Preprints are preliminary reports that have not undergone peer review.
They should not be considered conclusive, used to inform clinical practice,
or referenced by the media as validated information.

21st-century global urbanization drives disproportionate change beyond urban areas

Kanishka Narayan

kanishka.narayan@pnnl.gov

Pacific Northwest National Lab https://orcid.org/0000-0001-8483-6216

TC Chakraborty

Pacific Northwest National Laboratory https://orcid.org/0000-0003-1338-3525

Ryan McManamay

Baylor University https://orcid.org/0000-0002-5551-3140

Brian O'Neill

Pacific Northwest National Laboratory https://orcid.org/0000-0001-7505-8897

Pralit Patel

Joint Global Change Research Institute https://orcid.org/0000-0003-3992-1061

Chris Vernon

Pacific Northwest National Laboratory https://orcid.org/0000-0002-3406-6214

Marshall Wise

Pacific Northwest National Laboratory https://orcid.org/0000-0002-2718-0051

Jennie Rice

Pacific Northwest National Laboratory https://orcid.org/0000-0002-7833-9456

Article

Keywords:

Posted Date: October 27th, 2026

DOI: https://doi.org/10.21203/rs.3.rs-11365040/v1

License: This work is licensed under a Creative Commons Attribution 4.0 International License.
Read Full License

Additional Declarations: There is **NO** Competing Interest.

21st-century global urbanization drives disproportionate change beyond urban areas

Kanishka B. Narayan (*kanishka.narayan@pnnl.gov*) [i], TC Chakraborty[i] , Ryan A. McManamay[ii], Brian C. O Neill[i], Pralit Patel[i], Chris Vernon[i] ,Marshall Wise[i] and Jennie S. Rice[i]

i)Pacific Northwest National Laboratory, Richland, WA, 99354, USA

ii) Department of Environmental Science, Baylor University, Waco, TX, 76798, USA

Abstract - Urbanization is a critical anthropogenic process with largely irreversible effects on the Earth's surface. However, the implications of future urbanization for other land-dependent systems, through changes in land availability and prices, remain poorly understood, largely due to simplified modeling assumptions and static urbanization constraints. Here, we quantify the impacts of urban land dynamics with a factorial scenario design combined with enhancements to a global multisectoral economic equilibrium model. We simulate divergent scenarios combining urbanization pathways, socioeconomic changes, and bioenergy deployment levels. Across all scenarios, global changes in non-urban land types by 2100 are almost twice as large as urban land changes. This is because managed land losses from urbanization are offset by expansions elsewhere or increased investment in yield-enhancing technologies or higher imports. These changes can increase crop prices, with some regions seeing up to a 20% increase. These results show that urban land expansion can have an indirect footprint that is much higher and beyond the physically urbanized area.

Introduction

Urban land cover expansion is an important anthropogenic process with an irreversible effect on the Earth's surface. Moreover, the rapid historical expansion of urban areas is projected to continue into the future(Chakraborty, 2024). Of note, the United Nations projects that by 2050, 68% of the world's population will be living in urban areas (UN, 2018). Some projections of future urbanization suggest that by the end of the century ~3.52 million km^2 of the Earth's surface could be built-up (compared to ~0.5 million km^2 today)(Gao & O'Neill, 2020).

This rapid expansion of urban areas will likely affect other sectors since urban land typically expands at the expense of other types of land cover. In several countries, urban land is increasingly replacing the most productive cropland (Bren d'Amour et al., 2017; Seto et al., 2011). Such replacement would be expected to cause inflated crop and food prices in the future given the increasing scarcity of cropland. Urban land expansion has also been found to deplete natural land cover that can alter the terrestrial carbon cycle (McManamay et al., 2024; Seto et al., 2011, 2012). Moreover, under certain future scenarios, urban land cover could compete for investment with new land cover types such as bioenergy crops(Nyairo et al., 2022). Such changes could affect the prices of food and energy across the global economy. Thus, future urban land expansion is an important variable that should be accounted for when evaluating future economic and energy impacts of land use change.

While it is expected that urbanization will continue into the future, projections of urbanization remain highly uncertain. Chakraborty et al. (2014) compared multiple projections of future urbanization that use different models and sociodemographic assumptions (Chakraborty, 2024). These projections range from 0.5 million to ~3.5 million km^2 of future urban land by the end of the century (Chakraborty, 2024). Of these, Gao and O'Neill (Gao & O'Neill, 2019, 2020) produced the highest 2100 projection of urban land cover (up to 3.5 million km^2 by 2100) among the models analyzed, utilizing several socioeconomic factors and future projections of urban populations from the Spatially-Explicit, Long-term, Empirical City development (SELECT) model. On the other hand, He et al. produced more modest projections of urban land cover (1 million km^2 by 2100) that are parameterized using remotely sensed data of impervious land cover and more conservative assumptions regarding future urban population growth (He et al., 2023a, 2023b). These results highlight how varying sociodemographic assumptions and definitions of urban land can significantly impact urban land cover projections.

However, existing urbanization projections typically focus solely on urban land cover without accounting for its consequences for other types of land use. Addressing competing multisectoral demands for land is critical to holistically evaluating the cascading effects of urbanization on land allocation and food and energy prices. Models that do consider land competition, such as integrated assessment models (IAMs), have typically assumed static urban land cover, or modeled urban land dynamics with simple assumptions. For example, the IMAGE model calculates future urbanization only as a function of changing incomes (Stehfest et al., 2014), whereas models such as the Global Change Analysis Model (GCAM) and the AIM-CGE model hold future urban land constant (Fujimori et al., 2017). Presumably, many global multisectoral models were initially developed without dynamic urbanization since urban land area, as a proportion of the global terrestrial land surface, is relatively small and was assumed to play a minor role in land-based sectoral interdependencies.

Other studies targeted at specific land-atmospheric system processes have shown that urbanization has a large impact on physical system outcomes (Hao et al., 2023; Krayenhoff et al., 2018; Oleson et al., 2008; Oleson & Feddema, 2020). Examples include the urban heat island effect (Bornstein, 1968; Yang et al., 2016; Zhou et al., 2015) and impacts to crop production (Bren d'Amour et al., 2017; Krayenhoff et al., 2018; McManamay et al., 2024). For instance, Bren d'Amour et al. (2017) found that urban extensification compromised the most productive croplands, leading to non-linear impacts of urbanization on agricultural yields. A recent study highlighted the need for a fully multisectoral approach to the cascading implications of urban dynamics (McManamay et al. 2024). However, studies thus far have not focused on the downstream land price/demand impacts of dynamic urbanization. Indeed, integration of urbanization in an MSD model could explore feedbacks and second-order adaptations of other human systems to land competition, such as compensatory increases in agricultural lands, shifts in agricultural production, and land economic adaptations. Taken as a whole, existing research points to these secondary adaptations including land teleconnections, i.e. compensatory adjustments in distal areas for urban-induced losses in land producing agricultural commodities, as a significant research gap in understanding the multisector implications of changes in future urban land cover.

To help fill this research gap, we introduce an implementation of dynamic multisectoral responses to changes in urban land within GCAM. GCAM is a state-of-the-art multisector dynamics model that models the economic interactions between energy, land, and water system supplies and demands (Binsted et al., 2022; K. Calvin et al., 2019). Traditionally, GCAM has held urban land constant while other land types compete dynamically over the selected time horizon. Here, we modify the model to ingest exogenously derived dynamic urbanization pathways as land demands that must be met at each time step (at a water basin scale). This allows urbanization to influence the available land for other, non-urban land uses as well as the prices of all land types and commodities. Given the high range of uncertainty in future urban land demand discussed above, we consider multiple pathways of urban expansion paired with scenarios of socioeconomic change. And, since future urban land expansion will have consequences not only for land for food crops and unmanaged vegetation but also for newer land types such as bioenergy cropland, we include scenarios with high levels of demand for bioenergy. We compare our results to those of counterfactual scenarios that hold urban land constant. Our approach allows us to analyze the displacements of cropland and unmanaged land that occur because of increasing urbanization and to understand how land/crop management changes to meet demand for food and energy products. The latter can emerge as land-based teleconnections that are within and between regions. Since these changes in land competition manifest in GCAM as land price changes across the economy, we also analyze the price effects of these changing urbanization patterns.

Results

Projected net land change at global scales

Our scenarios at a global scale produce a wide range of outcomes when it comes to different land types as a result of the specified extents of urbanization (Figure 1). As mentioned in the methods section under the urbanization scenarios, the land allocation responses for all non-urban land types are calculated endogenously by GCAM.

Compared to the static urbanization scenario, the accelerating urbanization scenario combined with SSP5 with low bioenergy produces the largest reduction in global natural land cover, such as forests (a reduction of approximately 0.5 million km^2 by 2100) and grassland (a reduction of 1 million km^2 by 2100). The largest reductions in natural land cover by the end of the century are seen in the Yangtze basin in China (-110 thousand km^2), and the Missouri river basin in the USA (-50 thousand km^2). Under scenarios with low bioenergy deployment, there is greater loss of forest land in Southern South America (-16 thousand km^2 by 2100 under SSP5) and West Africa (-38 thousand km^2 by 2100 under SSP5) since the lack of a carbon price does not protect much forest from urban expansion. SI Figure 6 shows the reduction in unmanaged land cover by basin in 2100.

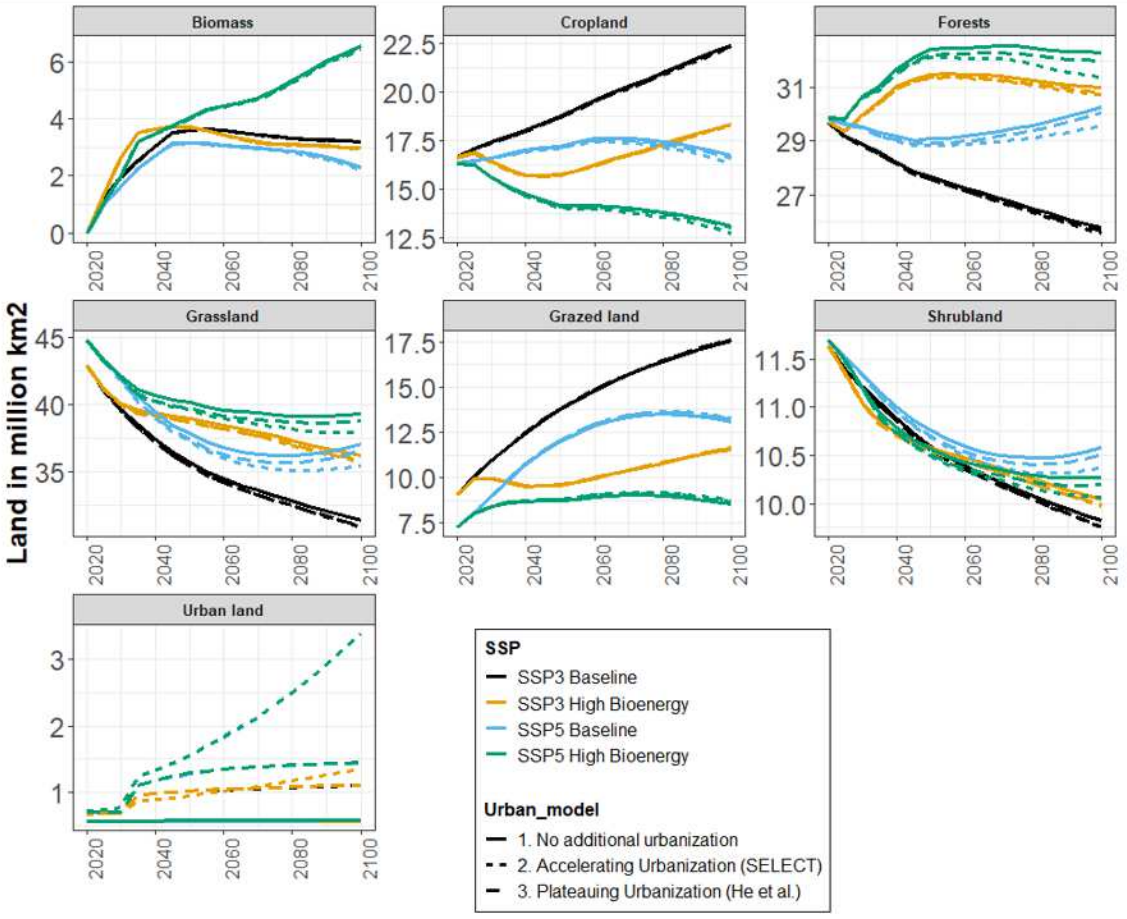


Figure 1: Global land cover evolution (2020 to 2100) for different land types by scenario and urbanization pathway in million km^2

Induced gross land change from urban expansion and emerging regional land teleconnections

Figure 2 shows the "gross" changes i.e. both positive and negative changes by land type that are directly caused by urban area expansion under each of the scenarios across all basins. As mentioned in the methods section, these are computed as the difference of land levels under a dynamic urban scenario compared to a counterfactual where urban land is held constant for the corresponding SSP and bioenergy assumptions. We can see that regardless of the levels of urbanization under the scenarios, there can be both increases and decreases in alternative land types due to increasing urbanization. We find that on average across scenarios globally, total land transitions from non-urban land are roughly 1.8 times the increase of urban land across scenarios. In terms of changes in managed lands this number is 0.9. SI Table 1 shows the changes in land for urban and non-urban land types. This shows that changing urbanization causes land removals (land directly displaced by urban land) as well as land replacements

(changes in land types to compensate for lost managed land) and the total effect of removal and displacements is disproportionate relative to the level of absolute urbanization.

At the basin scale, even though urbanization displaces cropland and drives the adoption of costlier land intensive technologies (such as irrigation) in a few specific basins; the more common response is shifting agricultural production to other basins entirely. Similar trends can also be observed for grazed land/grazed pasture. For example, while changing urbanization causes depletion of cropland and net natural lands (as seen in Figure 2), there are some basins where cropland, and especially irrigated cropland, increases rather than decreases. Figure 3 shows basins which experience increases in managed land cover under the urbanization scenarios. We can see that amongst these, there are a few basins which still see significant increases in urban land (e.g., ~20 thousand km^2 increase in Nile River Basin under the accelerating urbanization scenarios). In the case of the Nile River basin and the Missouri River

basin in the USA, there are increases not just in regular cropland but also irrigated cropland (e.g., ~10 thousand km^2 in the Nile River basin under SSP3).

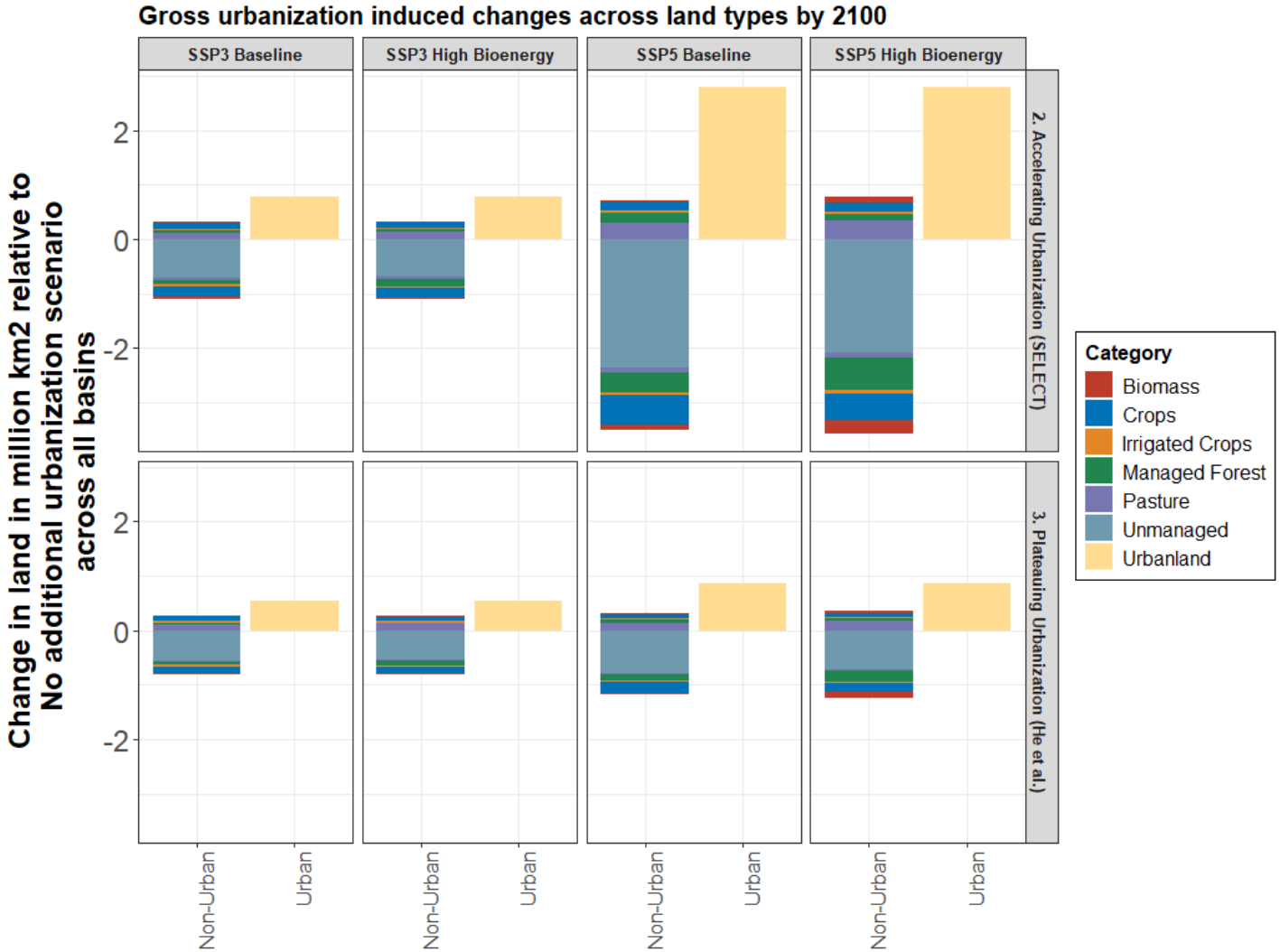


Figure 2: Gross global land use change across all basins in million km^2 under alternative urbanization scenarios (facets) and alternative SSP scenarios (x axis).

Several basins such as the RioPlata basin in South America, and water basins in Australia see large increases in unirrigated cropland due to increased urbanization. Under SSP5, increases are amplified given higher levels of demand. Similarly, when there are high levels of bioenergy production in the model, increases in crop expansion in these basins are higher. Moreover, several basins across Australia, South America, Africa see large increases in grazed land under all scenarios (SI Figure 7). When there is a high level of bioenergy production specified in the

model, there is less loss of unmanaged lands, especially in forests (since these scenarios are implemented though pricing of carbon). Thus, under these scenarios, there can be less loss of land to increased grazing in regions with high forest cover such as the Amazon in South America. But this is compensated for by increasing the levels of grazed land in basins without significant levels of forest cover (such as Australia).

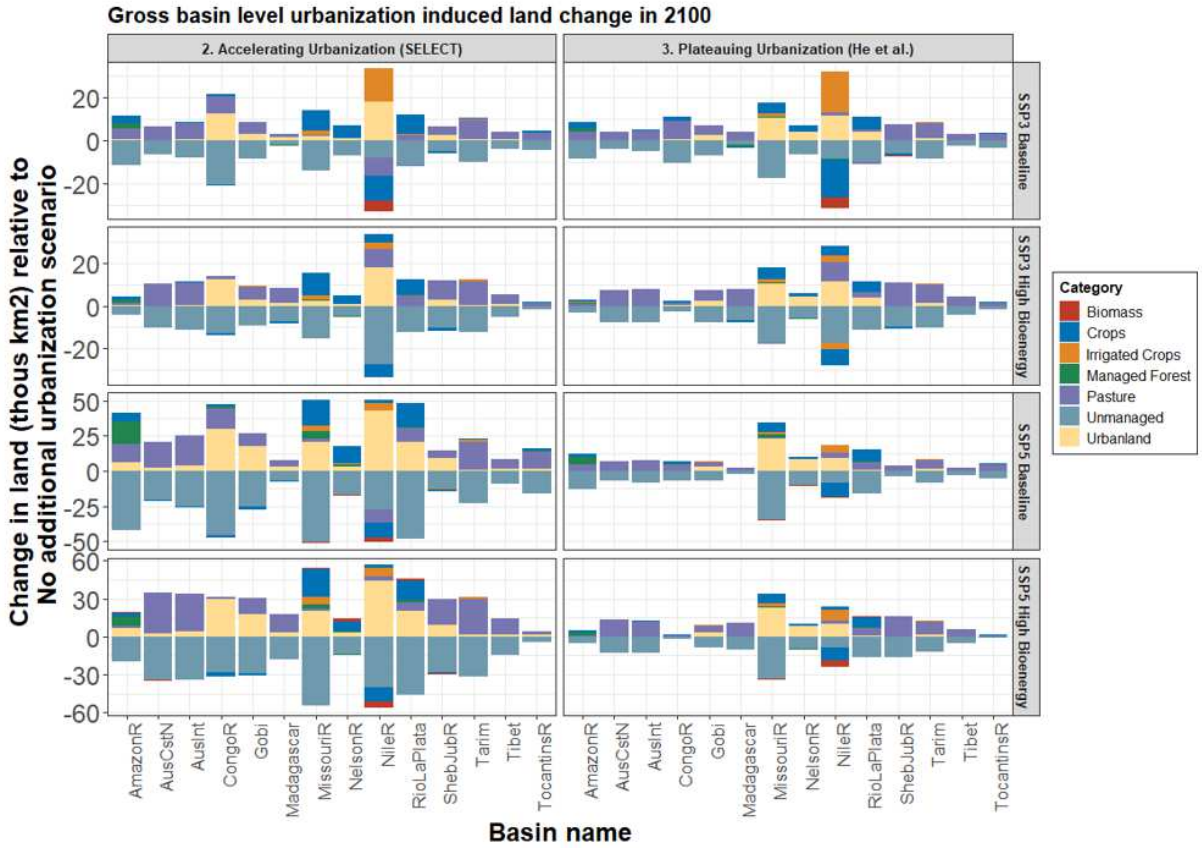


Figure 3: Gross urbanization-induced land change for selected basins across all scenarios. Basins are selected where managed land change exceeds 10 thousand km2 by 2100.

Figure 4 shows changes in total managed land (irrigated cropland + rainfed cropland + grazed land + managed forests) induced by urbanization across all basins in the world across all scenarios. In some regions such as India and Indonesia, managed land, especially cropland is generally reduced by 2100 across most basins across all scenarios with additional urbanization (reductions up to -90 thousand km2 by 2100). Consequently, these regions would have to rely more on imports rather than domestic production to meet demand. SI Figure 8 shows increase in imports of food and feed crops on account of increased urbanization across regions. By 2100, imports of rice in Indonesia can increase by up to 7% and imports of wheat in India can increase by up to 5%. Note that these increases are purely driven by urban land expansion which as mentioned above is still a small % of all regional land cover.

As discussed above, certain basins like the Missouri River Basin in the US and the Nile River basin see increases in cropland consistently across all scenarios. Similarly, in South America,

there is an increase in cropland in the Amazon basin in response to increasing urbanization on the basins on the east coast. However, under scenarios with high bioenergy deployment via carbon pricing, the increases in cropland in the Amazon River basin do not occur since these would lead to displacement of forests which would be valuable from a carbon perspective under these scenarios.

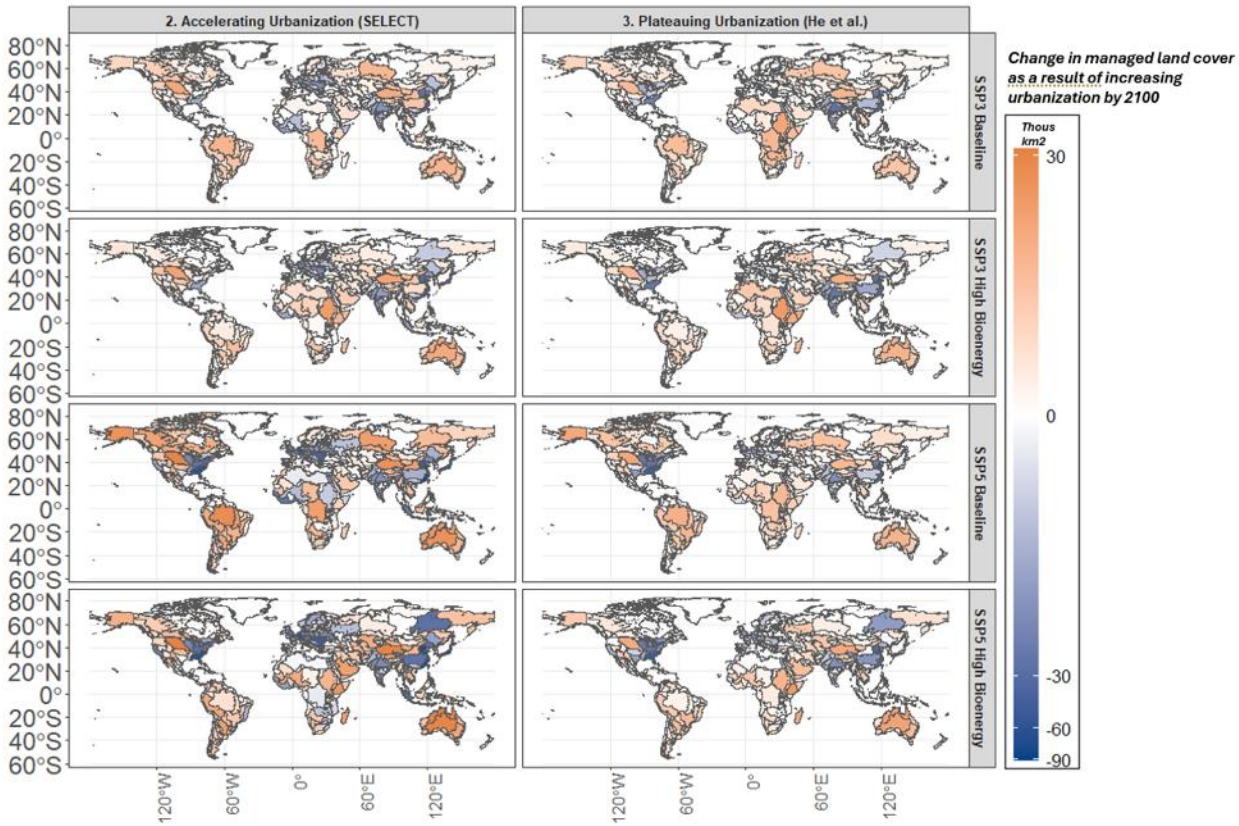


Figure 4: Change in total managed land cover in 2100 across all basins on account of increasing urbanization in thousand km2.

Thus, given the above we can conclude that with changing/increasing urbanization, the allocation of land shifts across basins to continue meeting demand for food and energy. This results in regional land-based teleconnections across basins where loss of managed land in one basin results in new managed lands in other basins or regions in response to urbanization. These teleconnections can take the form of increasing land allocation for costlier agricultural technologies (e.g. increase in irrigated cropland in the Nile, Missouri river basins), higher reliance on imports (such as India, Indonesia) or shifting of agriculture/grazed area to other productive basins (increases in grazed land in basins in Australia in response to higher demand for pasture products)

Change in prices and values of urban land

By comparing prices of urban land under any given scenario with the corresponding prices under a static urbanization scenario, we can calculate an urban price index (Urban PI) as the level of

change in prices of urban land as a direct result of urbanization (As explained in equation 1). SI Figure 5 shows the Urban PI in all years across all basins under every scenario and urbanization pathway compared with the rate of change in urban land cover itself. We find that the urban price changes are correlated with the rate of change of urban land across scenarios and urbanization pathways with R^2 values above 0.7. We note that prices share a non-linear relationship with changes in urban land, with changes in urban prices saturating with high levels of increase in urbanization. This largely follows price trends for land types in GCAM which show non-linear responses of prices due to larger increases reaching economies of scale. Prices of urban land are generally the highest in basins with high levels of bioenergy deployment with the "Accelerating urbanization" pathway producing large levels of price changes (e.g. urban price index of up to 30 in some basins under SSP5).

Consequently, regions experiencing massive urban expansion may not necessarily face proportional increases in urban land prices (e.g., 100 times increase in urban land only results in an urban price index of ~16). This is mainly because, in absolute terms, the amount of urban land increase is still relatively small relative to unmanaged and cropland (e.g., under SSP5 under the highest urban expansion scenario, global cropland in 2100 is estimated to be ~12 million km^2, grassland is estimated to be ~37 million km^2, but urban land cover is only 3.5 million km^2).

Effect of urbanization on commodity prices

The shifting patterns of land use and new regional teleconnections discussed above can cause changes in regional prices of different agricultural commodities. Similar to the urban price index, we calculate a crop price index to investigate how additional urban land expansion affects crop prices for individual types of crops (as seen in Equation 1). Figure 5 shows a distribution of these crop price indices across basins for different bioenergy and food crops. We observe that the highest increases in crop prices due to increasing urbanization occur under SSP5 with high bioenergy utilization. By 2100, wheat, corn, rice and soybean prices can be up to 20% higher in these cases. This is especially the case under the accelerating urbanization pathway although the plateauing urbanization pathway shows up to 5% increases on average in crop prices across basins by 2100.

However, there is significant heterogeneity in crop price effects across regions. In regions such as the US and China where agriculture shifts to other basins, crop prices can be higher by 10% (especially for forest products and wheat) in 2100 with an average increase of 7% across all crops, whereas for India (where urbanization leads to a general reduction in cropland across basins and more reliance on imports), the average increase is around 5% with soybeans seeing the largest increase. Amongst all crops, wheat generally sees the highest increase in prices in scenarios. This highlights that even though future urbanization projections are low in absolute terms, they can shift land allocations enough to significantly affect crop prices.

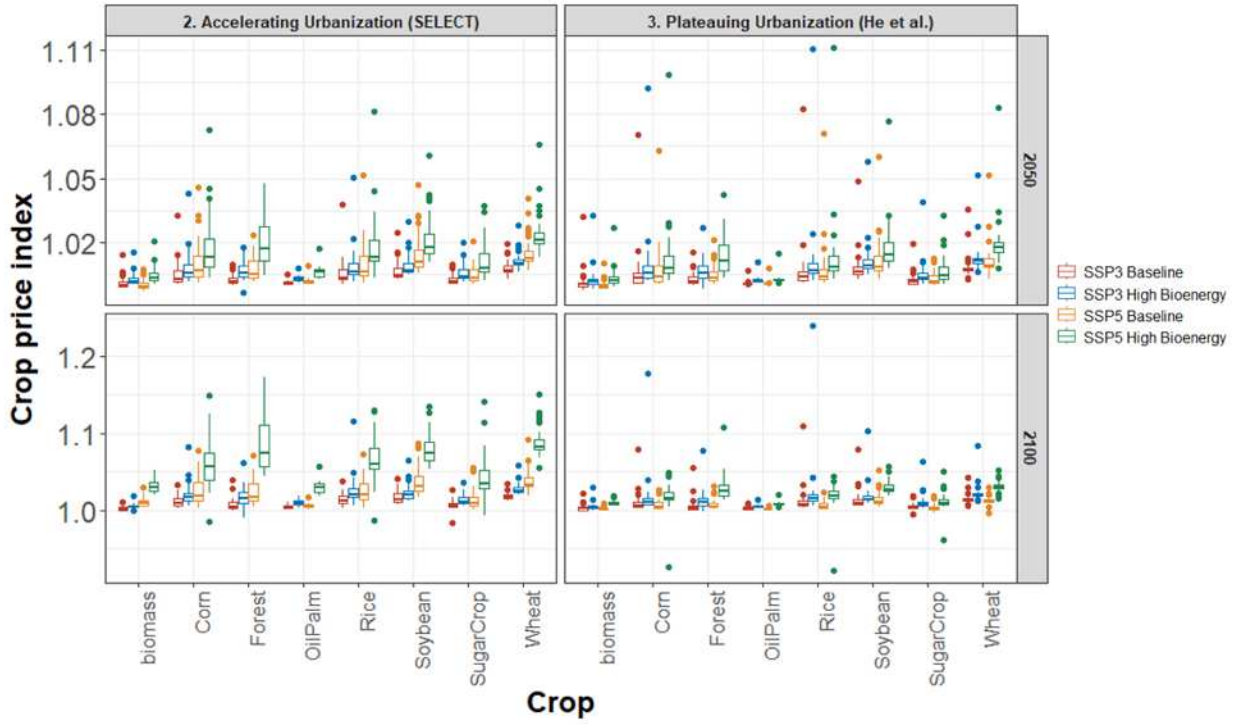


Figure 5: Crop price indices in 2050 and 2100 across urbanization pathways (facets) and socioeconomic scenarios (colors). Box plots represent distributions of prices across all economic regions in GCAM.

Discussion

In this paper, we implemented endogenous responses to urbanization within a detailed multisector dynamics partial equilibrium model to understand how urbanization can affect land allocation and crop prices within regions and across the economy. We used a factorial scenario design to explore alternative combinations of urbanization growth trends, socioeconomic change, and bioenergy deployment. Across these scenarios, we found that increases in urban land can cause disproportionate shifts in how land is managed across basins and significantly affect commodity prices.

To meet demands for food and energy under increasing urbanization, the land system responds in different ways across basins and regions. In some regions, there is a consistent shifting of cropland to other basins (such as the Missouri and Nile River basins) when there is loss of cropland elsewhere (e.g. Southeastern US). In some basins there is a shift towards irrigated agriculture, such as in the Nile River basin. Similarly, there is a systematic shift (across scenarios) of grazed land to some basins (e.g. basins in Australia). In some regions such as India and Indonesia, there can be reductions in cropland across all basins in response to urbanization and an increase in import of food and feed crops to meet future demand.

The total gross changes (positive + negative changes) in non-urban land areas in response to increasing urbanization are almost twice the total urban land change by 2100 across all scenarios. In addition to displacing unmanaged land and cropland, urban growth leads to changes in cropping to varying extents across scenarios. For example, under the SSP3 scenarios, there is an average increase of 600 thousand km2 of urban land by 2100 across all scenarios which leads to an average increase of 145 thousand km2 of additional cropland globally, 24% of the urban land increase. Under the SSP5 scenarios, there is an average increase of 1.8 million km2 of urban land by 2100 globally, with a corresponding increase in cropland of 200 thousand km2, 11% of the urban land increase. More importantly, these increases are heterogenous both within and between regions. In the US, by 2100, the largest increases in urban land are in the USA Southeast basin (+ 94 thousand km2), the Ohio river basin (+ 40 thousand km2), the Mississippi River basin (+ 38 thousand km2) and the California river basin (+ 34 thousand km2), while the basins with the highest increases in cropland are basins in the mid-west such as the Missouri River basin (+ 27 thousand km2).

Moreover, the analysis of price effects shows that even modest increases in urbanization (such as those seen under the plateauing urbanization scenarios) can increase regional crop prices by an average of 5% by 2100 and this increase can be up to 20% for some crops in some regions for some crops. This further confirms the disproportionate effect of increasing urban land on broader non-urban and economic systems. Moreover, scenarios combining urbanization with high levels of bioenergy deployment produce the highest effects on crop prices because the bioenergy scenario's carbon prices tend to protect natural lands, further reducing land available for crops.

Overall, we show the importance of examining and isolating land use change teleconnections related to urbanization, addressing the lack of holistic analysis across these kinds of models (McManamay et al. 2022). There are some caveats to our analysis that should be accounted for in the future. First, we model only a single type of urban land in GCAM, though there can be alternative ways in which urban land expands in the future (e.g., vertical vs horizontal expansion)(Soltani et al., 2025; Zambon et al., 2019). This could change the price effects we observe under these scenarios. We also rely on exogenous projections of urban land from other models in this study. While this allows us to analyze effects on land reallocation and price responses, this does not allow GCAM to adjust levels of urbanization in basins based on prices. In the future, the community should focus on developing urbanization demand functions that would contain such responses. The demand for urban land should also be connected to changes in other sectors, such as buildings and transportation, to further analyze effects on energy and water systems.

Finally, our analysis has important implications for Earth system models, where accounting for land re-allocation of cropland and grazed land on account of urbanization could alter Earth system model simulations. One area of future exploration is utilizing these results within urbanization models themselves. For example, further research could utilize the price effects as calculated here to inform spatial downscaling models to achieve economics-informed urbanization projections.

Methods

Implementation of dynamic urbanization response in GCAM

The Global Change Analysis Model (GCAM) is a detailed multisector dynamics model that represents the interactions between land, water, and energy systems. GCAM contains a detailed land model where several types of commercial and non-commercial land types compete for investment across 384 water basins globally (SI Figure 1 shows the map of the land regions in GCAM). The competition between land types in GCAM is based on a logit model of sharing based on relative inherent profitability of using land for competing purposes(K. Calvin et al., 2019; McFadden, 1972; Train, 2009). The efficacy of the land modeling equations in GCAM has been validated in the past using hindcast experiments(K. V. Calvin et al., 2022).

For this study, we modified GCAM's land module to include a dynamic urban land type which competes for investment against other land types based on a profit rate. To represent the uncertainty in future urban land demand, we then impose exogenous alternative pathways of dynamic demands for urban land at the basin scale (see next section for description of urbanization pathways) based on projections from other models. GCAM then competes all other land types for investment based on the demand for urban land and the demand for other commodities such as food and energy. This allows the model to compute price effects due to changing urbanization competing against food and energy demands. Note that even though the demand for urban land is exogenous, the model still endogenously calculates prices of urban land. Thus, the urban land price is a result of endogenous supply response combined with exogenous demand quantity.

Urban lands are initially assigned an economic value/profit rate that is equal to the value of cropland. In the calibration years (1975-2015), the model considers the changing levels of historical urban land, cropland and other land types to calculate all economic parameters (e.g. elasticities) such that all land types are in equilibrium in the final calibration year. In future years (i.e. 2020 onwards) the value of urban land can increase over time as the demand for urban land increases. As urban land demands change, GCAM endogenously models the resultant effect on urban and non-urban land prices based on economic land competition stemming from expected profits. Historical land use and land cover in GCAM are initialized using pixel scale data aggregated to the basin scale for several management types, vegetation types.

In GCAM, competing uses of land are nested within land nodes (SI Figure 2 shows a simple description of existing land nodes with different land types). Within each land node, it is generally assumed to be easier to substitute land uses within nodes rather than whole land nodes. Examples include switching food crops from one to another and converting forests from unmanaged categories to logging forests. Substitution across land nodes is also allowed but is assumed to be more difficult than within land nodes. Urban land in GCAM is classified under the cropland node. Thus if urban land increases in GCAM, it is easier for the model to displace cropland rather than unmanaged land (e.g. forests or grasslands), which follows findings from previous studies(Bren d'Amour et al., 2017; Seto et al., 2012). Ultimately, the decision of how much natural or unmanaged land versus cropland is displaced is determined by prices and profits. GCAM includes technological options for intensified agriculture (e.g. irrigated agriculture with higher yields), so as future urban land cover increases, the model can respond

through more intensified agriculture based on prevalent prices and demand. Additionally, since GCAM will maintain economic equilibrium across all sectors, increasing urbanization will be compensated for by second-order adjustments in other sectors in the land system and the overall economy in GCAM. Finally, these changes will manifest in the model as changes in prices not just of urban land but also all other land types. SI Figure 3 summarizes the updates made to include endogenous urbanization responses in GCAM.

Scenario structure

As described above there are a wide variety of urban land projections available in the literature (ranging from 0.5 million km2 to 3.5 million km2 globally by 2100). These projections are influenced by socioeconomic factors such as future population and income growth and the definition of urbanization. We impose two distinct urbanization pathways (to represent high and low projections of urbanization) in this study to understand the effect of future urbanization on land competition and resultant prices.

A) An **Accelerating Urbanization** pathway simulated by SELECT which models future urbanization including all built up areas (dense urbanization and exurban expansion) and results in total maximum global urban land cover of 3.5 million km2 by 2100. The increases in urbanization under this scenario are generally uniform across all regions with significant heterogeneity at the basin scale.
B) A **Plateauing Urbanization** pathway from He et al. which is based on remote sensing data of impervious surfaces. This pathway results in a maximum urbanization of 1.5 million km2 globally by 2100, but with high levels of urbanization in the global north in particular.

We pair each of these pathways with two socioeconomic scenarios (van Vuuren et al., 2017), namely SSP3, which represents high regional rivalry (i.e. less trade) and a more constrained land system, and SSP5, which represents high levels of per capita income growth which leads to more urbanization. This gives four alternative demand projections of urban land expansion. These demand pathways are calculated at the pixel scale and then specified for each water basin separately (SI Figure 4 shows increases in urban land across all basins by 2100).

We further pair our dynamic urbanization-socioeconomic scenarios with two scenarios of demand for bioenergy crops: low and high. The low case is based on the projected baseline demand for bioenergy The high case bioenergy demands are simulated using a carbon price which forces GCAM to reach a radiative forcing level of 2.6 W/m^2 by 2100. This is important since bioenergy crops will also compete for investment with future urban land against the other land types. As a result of the inherent carbon price, the bioenergy deployment scenarios also have the effect of protecting more natural lands from expansion.

This gives us a total of eight scenarios for dynamic urbanization. We also construct four scenarios for static urban land by pairing the two socioeconomic scenarios with the two bioenergy scenarios. The static urban land scenarios will help us isolate the effect of dynamic

urbanization (see section below). Figure 6 shows how we build our twelve scenarios using the above-mentioned variables.

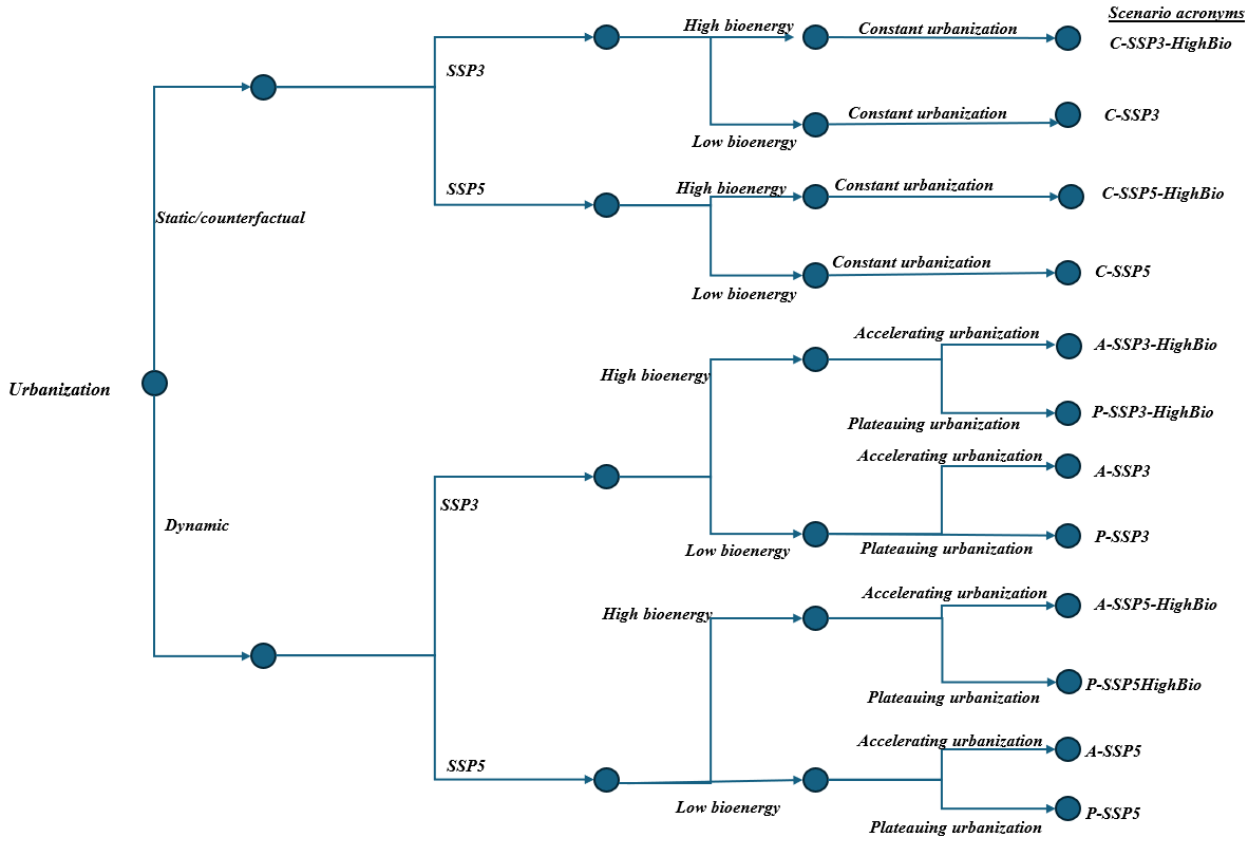


*Figure 6: Plot showing scenario construction for the scenarios used in this analysis. Last column describes scenario acronyms which are combinations of the urbanization models (Constant(**C**), Accelerating(**A**), Plateauing(**P**)), SSPs (**SSP3**, **SSP5**), Bioenergy parameterization (**HighBio**)*

Computing the effect of changing urbanization on outcome variables

We compute the effect of changing urbanization on urban land commodity prices/values by comparing the land change/price change under a given dynamic urban scenario with the counterfactual scenario (where future urban land does not change) that has the same socioeconomic and bioenergy assumptions. This approach allows us to compute a price index (for any commodity) which responds only to changing urbanization, that is, the price index is 1 when urbanization is not changing. Thus, if the index value is 2 in any given time step, it means prices have doubled on account of changing urbanization. Equation (1) summarizes the calculation of the urban price index:

$$PI_{b,t,s,u,c} = (P_{b,s,t,u,c})/(P_ConstantUrbanization_{b,s,t,c}) \quad (1)$$

Where,

PI is the calculated index which is unitless.

P is the price of urban land or any commodity in $/km2.

b is one of the 384 water basins in GCAM.

s is the SSP scenario combined with bioenergy parameterization

u is one of the 3 urbanization pathways described above (i.e., static or 2 variants of dynamic urbanization).

t is the timestep

c is the commodity i.e. urban or any crop/bioenergy commodity

Funding statement

This research was supported by the U.S. Department of Energy, Office of Science, as part of research in MultiSector Dynamics, Earth and Environmental System Modeling Program (Grant No. 59534).

Data and code availability

All data used in this study along with code for replication and replication instructions are available at this repository- https://zenodo.org/records/23169192 and the version of GCAM used for the analysis is available here- https://github.com/JGCRI/gcam-dev/tree/kbn_dynamic_urban.

Author contributions

KBN, TC, RM, BCO, JSR conceived the study design. KBN performed the analysis. All authors contributed equally in the writing of the manuscript. TC, RM, JSR provided detailed comments on early drafts.

References

Binsted, M., Iyer, G., Patel, P., Graham, N. T., Ou, Y., Khan, Z., Kholod, N., Narayan, K., Hejazi, M., Kim, S., Calvin, K., & Wise, M. (2022). GCAM-USA v5.3_water_dispatch: Integrated modeling of subnational US energy, water, and land systems within a global framework. *Geoscientific Model Development*, *15*(6), 2533–2559. https://doi.org/10.5194/gmd-15-2533-2022

Bornstein, R. D. (1968). Observations of the urban heat island effect in New York City. *Journal of Applied Meteorology and Climatology*, *7*(4), 575–582.

Bren d'Amour, C., Reitsma, F., Baiocchi, G., Barthel, S., Güneralp, B., Erb, K.-H., Haberl, H., Creutzig, F., & Seto, K. C. (2017). Future urban land expansion and implications for global croplands. *Proceedings of the National Academy of Sciences*, *114*(34), 8939–8944. https://doi.org/10.1073/pnas.1606036114

Calvin, K., Patel, P., Clarke, L., Asrar, G., Bond-Lamberty, B., Cui, R. Y., Di Vittorio, A., Dorheim, K., Edmonds, J., Hartin, C., Hejazi, M., Horowitz, R., Iyer, G., Kyle, P., Kim, S., Link, R., McJeon, H., Smith, S. J., Snyder, A., … Wise, M. (2019). GCAM v5.1: Representing the linkages between energy, water, land, climate, and economic systems. *Geoscientific Model Development*, *12*(2), 677–698. https://doi.org/10.5194/gmd-12-677-2019

Calvin, K. V., Snyder, A., Zhao, X., & Wise, M. (2022). Modeling land use and land cover change: Using a hindcast to estimate economic parameters in gcamland v2.0. *Geoscientific Model Development*, *15*(2), 429–447. https://doi.org/10.5194/gmd-15-429-2022

Chakraborty, T. (2024). *Large disagreements in estimates of urban land across scales and their implications* (p. 5922316249 Bytes) [Dataset]. figshare. https://doi.org/10.6084/M9.FIGSHARE.25225535

Fujimori, S., Hasegawa, T., & Masui, T. (2017). AIM/CGE V2.0: Basic Feature of the Model. In S. Fujimori, M. Kainuma, & T. Masui (Eds.), *Post-2020 Climate Action* (pp. 305–328). Springer Singapore. https://doi.org/10.1007/978-981-10-3869-3_13

Gao, J., & O'Neill, B. C. (2019). Data-driven spatial modeling of global long-term urban land development: The SELECT model. *Environmental Modelling & Software*, *119*, 458–471. https://doi.org/10.1016/j.envsoft.2019.06.015

Gao, J., & O'Neill, B. C. (2020). Mapping global urban land for the 21st century with data-driven simulations and Shared Socioeconomic Pathways. *Nature Communications*, *11*(1), 2302. https://doi.org/10.1038/s41467-020-15788-7

Hao, L., Sun, G., Huang, X., Tang, R., Jin, K., Lai, Y., Chen, D., Zhang, Y., Zhou, D., & Yang, Z.-L. (2023). Urbanization alters atmospheric dryness through land evapotranspiration. *Npj Climate and Atmospheric Science*, *6*(1), 149.

He, W., Li, X., Zhou, Y., Shi, Z., Yu, G., Hu, T., Wang, Y., Huang, J., Bai, T., Sun, Z., Liu, X., & Gong, P. (2023a). *Global fractional urban changes at 1km under diverse SSP-RCP scenarios throughout 2100* (p. 1851123604 Bytes) [Dataset]. figshare. https://doi.org/10.6084/M9.FIGSHARE.20391117.V4

He, W., Li, X., Zhou, Y., Shi, Z., Yu, G., Hu, T., Wang, Y., Huang, J., Bai, T., Sun, Z., Liu, X., & Gong, P. (2023b). Global urban fractional changes at a 1 km resolution throughout 2100 under eight scenarios of Shared Socioeconomic Pathways (SSPs) and Representative Concentration Pathways (RCPs). *Earth System Science Data*, *15*(8), 3623–3639. https://doi.org/10.5194/essd-15-3623-2023

Krayenhoff, E. S., Moustaoui, M., Broadbent, A. M., Gupta, V., & Georgescu, M. (2018). Diurnal interaction between urban expansion, climate change and adaptation in US cities. *Nature Climate Change*, *8*(12), 1097–1103. https://doi.org/10.1038/s41558-018-0320-9

McFadden, D. (1972). *Conditional logit analysis of qualitative choice behavior*. https://escholarship.org/content/qt61s3q2xr/qt61s3q2xr.pdf

McManamay, R. A., Vernon, C. R., Chen, M., Thompson, I., Khan, Z., & Narayan, K. B. (2024). Dynamic urban land extensification is projected to lead to imbalances in the global land-carbon equilibrium. *Communications Earth & Environment*, *5*(1), 70. https://doi.org/10.1038/s43247-024-01231-y

Nyairo, R., Hasegawa, T., Fujimori, S., Wu, W., & Takahashi, K. (2022). Socio-economic trajectories, urban area expansion and ecosystem conservation affect global potential supply of bioenergy. *Biomass and Bioenergy*, *159*, 106426. https://doi.org/10.1016/j.biombioe.2022.106426

Oleson, K. W., Bonan, G. B., Feddema, J., Vertenstein, M., & Grimmond, C. S. B. (2008). An urban parameterization for a global climate model. Part I: Formulation and evaluation for two cities. *Journal of Applied Meteorology and Climatology*, *47*(4), 1038–1060.

Oleson, K. W., & Feddema, J. (2020). Parameterization and Surface Data Improvements and New Capabilities for the Community Land Model Urban (CLMU). *Journal of Advances in Modeling Earth Systems*, *12*(2), e2018MS001586. https://doi.org/10.1029/2018MS001586

Seto, K. C., Fragkias, M., Güneralp, B., & Reilly, M. K. (2011). A Meta-Analysis of Global Urban Land Expansion. *PLoS ONE*, *6*(8), e23777. https://doi.org/10.1371/journal.pone.0023777

Seto, K. C., Güneralp, B., & Hutyra, L. R. (2012). Global forecasts of urban expansion to 2030 and direct impacts on biodiversity and carbon pools. *Proceedings of the National Academy of Sciences*, *109*(40), 16083–16088. https://doi.org/10.1073/pnas.1211658109

Soltani, A., Azizi, P., Rahimioun, A., & Sedaghatfard, M. (2025). Volumetric urban sprawl: Horizontal and vertical growth in two metropolitans. *Journal of Urban Management*. https://www.sciencedirect.com/science/article/pii/S2226585625000433

Stehfest, E., van Vuuren, D., Bouwman, L., & Kram, T. (2014). *Integrated assessment of global environmental change with IMAGE 3.0: Model description and policy applications*. Netherlands Environmental Assessment Agency (PBL). https://dspace.library.uu.nl/bitstream/handle/1874/308545/PBL_2014_Integrated_Assessment_of_Global_Environmental_Change_with_IMAGE_30_735.pdf

Train, K. E. (2009). *Discrete choice methods with simulation*. Cambridge university press. https://books.google.com/books?hl=en&lr=&id=4yHaAgAAQBAJ&oi=fnd&pg=PR7&dq=Train+K+E+2009+Discrete+Choice+Methods+with+Simulation+(Cambridge+University+Press)&ots=eG29Fbf1fu&sig=sQK3YN5T36-O9SE8nvk5jEUkzeQ

UN. (2018). *68% of the world population projected to live in urban areas by 2050, says UN | UN DESA | United Nations Department of Economic and Social Affairs*. https://www.un.org/development/desa/en/news/population/2018-revision-of-world-urbanization-prospects.html

van Vuuren, D. P., Kriegler, E., Edmonds, J., O'Neill, B. C., Fujimori, S., Bauer, N., Calvin, K., Dellink, R., Fricko, O., Lutz, W., Popp, A., Cuaresma, J. C., Kc, S., Leimbach, M., Jiang, L., Kram, T., Rao, S.,

Emmerling, J., Ebi, K., … Tavoni, M. (2017). The Shared Socioeconomic Pathways and their energy, land use, and greenhouse gas emissions implications: An overview. *Global Environmental Change*, *42*, 153–168. https://doi.org/10.1016/j.gloenvcha.2016.05.009

Yang, L., Qian, F., Song, D.-X., & Zheng, K.-J. (2016). Research on urban heat-island effect. *Procedia Engineering*, *169*, 11–18.

Zambon, I., Colantoni, A., & Salvati, L. (2019). Horizontal vs vertical growth: Understanding latent patterns of urban expansion in large metropolitan regions. *Science of the Total Environment*, *654*, 778–785.

Zhou, D., Zhao, S., Zhang, L., Sun, G., & Liu, Y. (2015). The footprint of urban heat island effect in China. *Scientific Reports*, *5*(1), 11160.

Supplementary Files

This is a list of supplementary files associated with this preprint. Click to download.

- GCAMUrbanizationpaperSI.pdf